



3D Inkjet Printer Nozzle Design: Performance Evaluation for Printable Electronics Applications

Mostafa Salehikhah¹, Samira Rezaei^{2*}, Milad Yousefzad³, Farzaneh Abooei Mehrizi⁴, Ramin Mir Mohammadi⁵, Negin Manavizadeh⁶, and Alireza Khodayari⁷

¹Tehran Central Branch, Islamic Azad University, Tehran, Iran, (ORCID:0009-0006-8313-6131),
m.salehikhah@yahoo.com

² Nanostructured-electronic Devices Laboratory, Faculty of Electrical Engineering, K. N. Toosi University of Technology, Tehran, Iran, (ORCID: 0000-0001-9864-6923), s.rezaei1@email.kntu.ac.ir

³Nanostructured-electronic Devices Laboratory, Faculty of Electrical Engineering, K. N. Toosi University of Technology, Tehran, Iran, (ORCID: 0000-0002-5001-0472), yousefzad@email.kntu.ac.ir

⁴Nanostructured-electronic Devices Laboratory, Faculty of Electrical Engineering, K. N. Toosi University of Technology, Tehran, Iran(ORCID: 0009-0003-2379-0180), farzanehabooei@email.kntu.ac.ir

⁵Faculty of Civil and Environmental Engineering, Amirkabir University of Technology, Tehran, Iran, (ORCID: 0009-0000-1298-2054), ramin1377@aut.ac.ir

⁶ Nanostructured-electronic Devices Laboratory, Faculty of Electrical Engineering, K. N. Toosi University of Technology, Tehran, Iran(ORCID: 0000-0001-8452-8627), manavizadeh@kntu.ac.ir

⁷Tehran Central Branch, Islamic Azad University, Tehran, Iran, (ORCID: 0000-0002-7237-1180),
a.khodayari@iauctb.ac.ir

(Received date: 01.12.2024, Revised date: 04.01.2024 and Accepted date: 15.02.2024)

(DOI: 10.29228/JCHAR.73959)

Corresponding Author: Samira Rezaei, Nanostructured-electronic Devices Laboratory, Faculty of Electrical Engineering, K. N. Toosi University of Technology, Tehran, Iran, s.rezaei1@email.kntu.ac.ir

CITE: M. Salehikhah, S. Rezaei, M. Yousefzad, F. A. Mehrizi, R. M. Mohammadi, N. Manavizadeh, and A. Khodayari, "3D Inkjet Printer Nozzle Design: Performance Evaluation for Printable Electronics Applications"*JCharacterization*, vol. 4, no. 1, 10-20, February, 2024, doi:10.29228/JCHAR.73959

Abstract

In recent times, inkjet printing technology has garnered considerable attention among professionals and researchers across various fields, including material engineering, biology, chemistry, electronics, and medicine. With its capacity to print diverse materials with remarkable precision and speed, this technology has found significant utility in the additive manufacturing process. The primary objective is to replace conventional coating methods such as lithography while adhering to established standards and maintaining the quality of previous techniques. Achieving this goal necessitates establishing a seamless synergy between the chosen mechanical structure and materials.

A significant challenge in 3D printing lies in fabricating intricate geometries, addressed by employing support structures that are removed once the printing is completed. These supports can be printed using dissolvable materials. The structural complexity is exacerbated by the process of constructing layers using separate print heads, triggering the expulsion of ink from the nozzle. The formation of distinct droplets is contingent upon the viscosity of the ink and its adherence to specific parameters. Successful printing of various materials relies on achieving optimal viscosity and resistance characteristics of the ink.

The paper also demonstrates the utilization of heater and ultrasonic technologies to expand the range of printable materials. This versatile technology accommodates a broad array of materials, including nanoparticles, cells, polymers, and pigments that can be either dissolved or dispersed within a fluidic medium. Furthermore,

incorporating conductive ink into this technology opens up potential applications in the field of printable electronics. In three parts we demonstrate the conductivity of ABS polymer, next we study the printability of ink and finally we simulate the deposited layer to find out the conductivity of it. We found out that ABS is conductive and our ink is printable and the deposited layer is conductive as well.

Keywords: 3D printing, dissolvable materials, printable electronics, nozzle

1. Introduction

3D printing is considered an additive manufacturing (AM) technique for fabricating a large scope of devices and instruments. Since the development of this technology by Charles Hull, several manufacturing methods such as powder bed fusion, fused deposition modeling (FDM), inkjet printing, and contour crafting (CC) have been deployed subsequently [1],[2].

3D printing can revolutionize different industries by facilitating cost-effective customization, complex geometries, and sustainable manufacturing processes. It suggests cost-effective and labor-free manufacturing, the use of recycled materials, and the possibility of an on-site manufacturing process [3]. This technology has the potential to minimize waste, serve as an affordable prototyping technique, and can be used to meet the specific demands of customers, such as the fabrication of medical implants based on CT-imaged tissue replicas.

Various methods of additive manufacturing have been developed to cater to the diverse requirements of different industries. These methods are fused deposition modeling (FDM), selective laser sintering (SLS), selective laser melting (SLM), inkjet printing, contour crafting, stereolithography (SLA), powder bed fusion, direct energy deposition (DED) and laminated object manufacturing (LOM) [1]. This paper presents an inkjet printing method for producing tools and devices such as electrodes. This method is well suited for printing complex structures; nevertheless, the printed object requires post-processing heat treatment.

Generally, implementing temperature sintering in inkjet printing enhances the mechanical performance of printed objects. Ultraviolet (UV) curing is another way of treating printed material with solidifying materials on demand. UV curing can be used in 3D printing pharmaceutical tablets to build scaffolds and complex (torus) tablet geometries with extended-release profiles at ambient temperature [3].

There are two main modes of inkjet printers: Drop on demand (DoD) mode and continuous mode (Figure 1). In DoD, single drops of ink are released onto a wide range of substrates in response to digital signal or waveform. This method offers high placement accuracy, controllability, and efficient material usage [4]. The 3D printing device in this work is based on DoD and it is operated with a Computer Numerical Control (CNC) machine along the 3-axis (x,y,z) with 0.05 mm precision. In continuous mode, continuous stream of ink is produced and drops break up from the print head nozzle by applying harmonic modulation. When compared to continuous inkjet technology, the DoD method not only consumes less ink but also provides superior placement accuracy. Also, the DoD method enables the printing of both aqueous and UV-curable inks. It uses low temperatures, making it ideal for printing water-based inks and expanding its application in inkjet-printed electronics. Ease of fabrication is an important factor in the design and implementation of electronic devices based on metal oxide semiconductors [5-10]. Inkjet printing technology can assist the fabrication process of electronic sensors, solar cells, transistors, and other electronic devices based on metal, metal oxide semiconductors, and nanostructures by enhancing material deposition based on printable inks. These inks could be used as contact electrodes or active layers on the device [11-16].

Different inkjet printing methods can be classified according to the type of inkjet printing technology employed. It is understood according to Figure 2 that there is an emphasis on piezoelectric inkjet technology. This mechanism utilizes a piezo-driven inkjet printhead, which is activated by applying a voltage waveform to a piezoelectric membrane, ensuring the precise formation of the desired droplet and a consistently stable jet. Challenges are hindering the utilization of piezoelectric inkjet printing technology such as nozzle clogging, noaxisymmetric effects, jet stability, printing speed, printing quality, and viscosity control [17],[19].

A wide range of materials can be utilized for the additive manufacturing technique. These materials include polymers, metals, and ceramics. The main methods for metal 3D printing are selective laser sintering (SLS), selective laser melting (SLM), and directed energy deposition (DED). Polymers like acrylonitrile-butadiene-styrene (ABS), polyamide (PA), polycarbonate (PC), and polylactic acid (PLA) are widely used in 3D printing. They are mainly used for fast prototyping, but recent developments have introduced the reinforcement of polymers with fibers and nano-materials to enhance their mechanical properties. Limited materials can be an issue in ceramic 3D printing. It is worth mentioning the possibility of utilizing 3D printing in large-scale structures through concrete 3D printing [3].

Nanomaterials such as nano SiO₂, carbon nanotubes, and quantum dot nanoparticles can be used in different 3D printing techniques to improve the mechanical properties, reinforcement effect, and optical properties of the printed parts [17]. Materials such as silver nanoparticles (AgNP), single-wall carbon nanotubes (SWCNTs), and

graphene are examples of materials that due to their respective properties such as high conductivity, being ability to print onto flexible substrates and the ability to be printed on thin layers are employed as conductive materials in printable electronics [4]. Some electronic-based applications of 3D printing are as follows: prototyping and product development, customized electronics (e.g., patient-specific devices and implants), embedded electronics, microelectronics and microfluidics, conductive and functional materials, and educational applications [3]. Innovative approaches to fabricating electronic devices can be explored by harnessing the advantages of inkjet printing, which include efficiency, design flexibility, post-processing options, a wide range of materials, and high resolution.

An example of fabricating multi-electrode arrays (MEAs) with inkjet printing for the study of cellular phenomena in vitro has been studied in [20]. This paper used PEDOT-PSS (poly(3,4-ethylenedioxythiophene): polystyrene sulfate) as the sole conductive material in the pMEAs. It is inkjet-printed onto the PI substrate to create conductive tracks, contact pads, and electrodes. This material showed low impedance, biocompatibility, and flexibility. Finally, the method used in this paper implementing inkjet printing offers a cost-effective, easy-to-pattern, flexible, customized, and high-resolution method for fabricating electrodes.

Support materials are as important as 3D printing materials in the total outcome of the system. The choice of support material depends on factors such as the printing technology, the material being printed, and the desired level of support and ease of removal. Some common support materials used in 3D printing include Water-soluble support materials, breakaway support materials, support materials with similar properties, and dissolvable support materials [4],[18].

In this work, an innovative 3D printer design is introduced, combining the principle of a 3-axis CNC machine with the functionality of an inkjet printer. This design incorporates two nozzles, one for dispensing ink and the other for dispensing support material (see Figure 3).

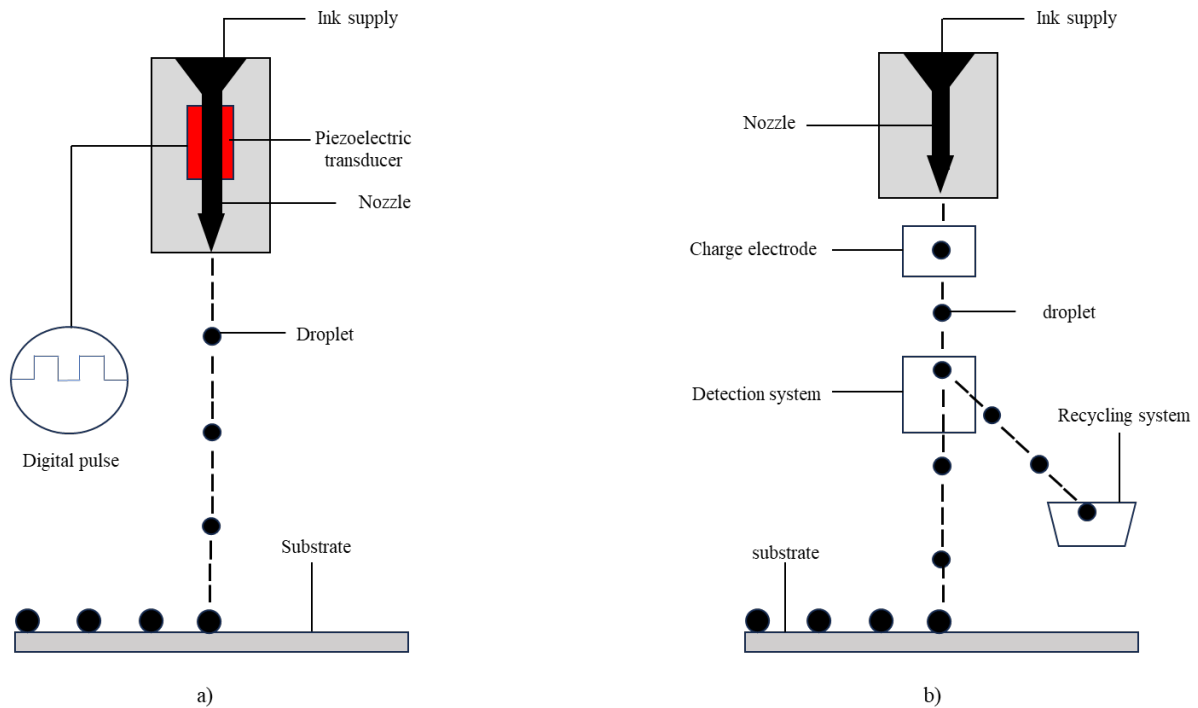


Figure 1: In DoD mode, the droplets are induced by a piezoelectric actuator (a), and in continuous inkjet printers, a continuous electro-conductive stream of fluid is delivered through a nozzle because of piezoelectric actuator vibrations, regulating the breakup of the stream into individual uniform droplets with uniform spacing (b) [3].

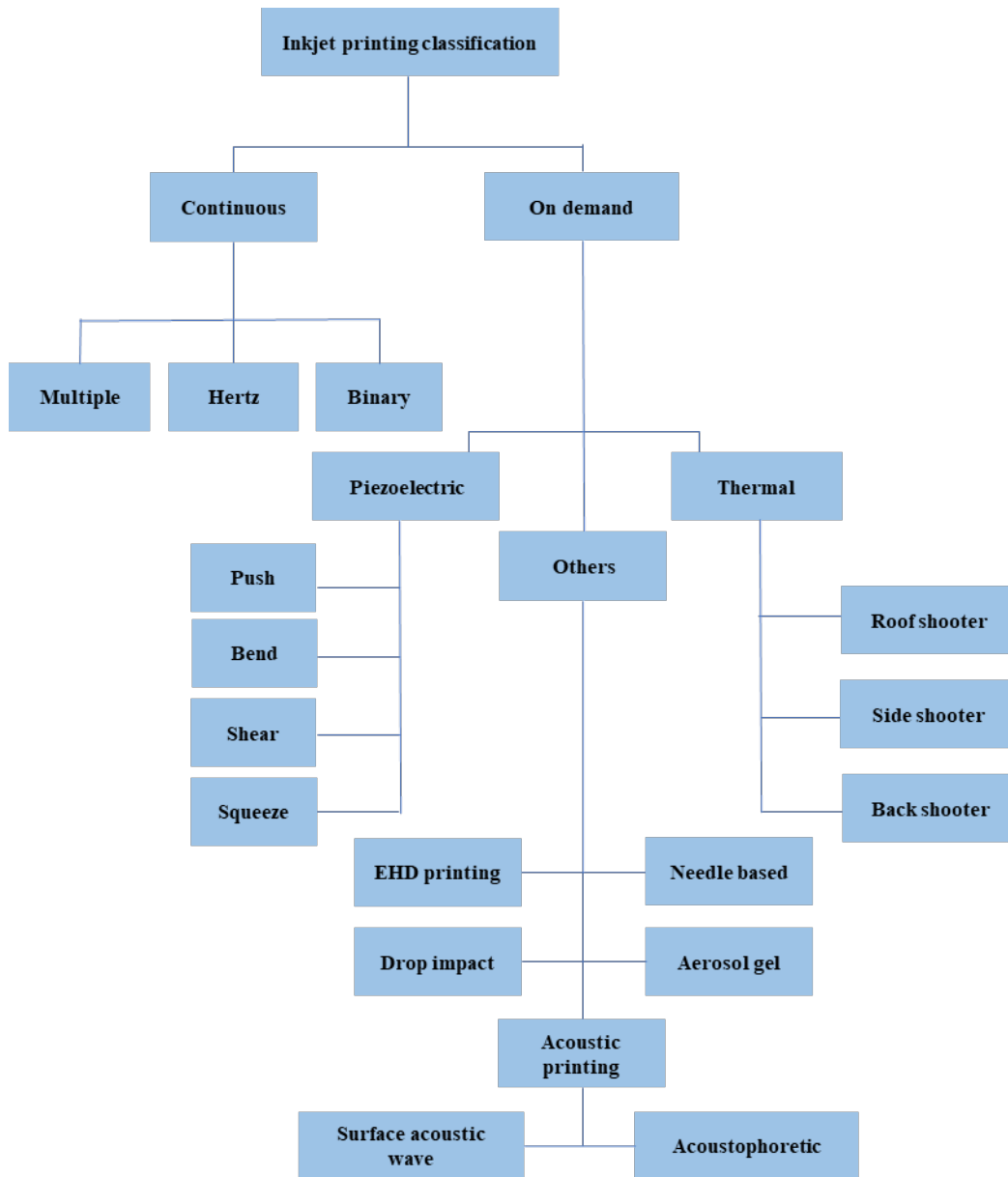


Figure 2: Classifications of Printing Technologies [21].

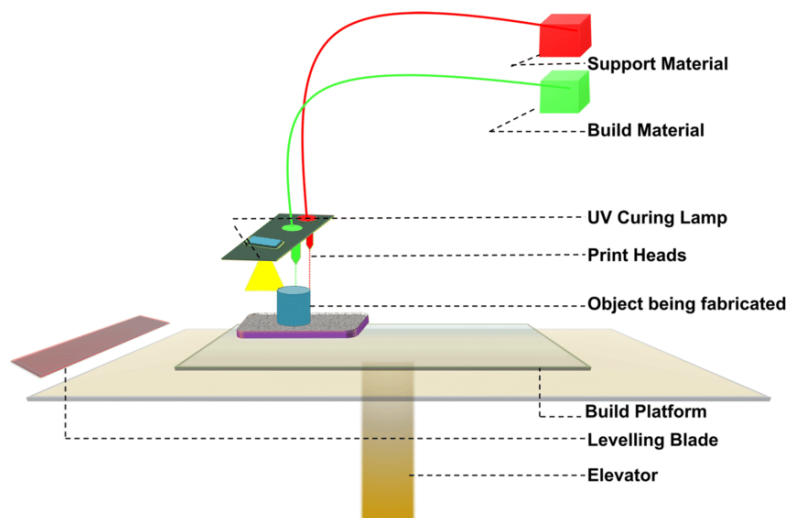


Figure 1: Schematic of Employing Two Nozzles in 3D Printers [21].

To assess the printing capability of the ink, it is crucial that the ink consistently emerges from the nozzle in a fixed shape at all times. Any variation in the amount of ink expelled from the nozzle leads to an uneven diameter of the cover layer on the substrate, causing the printing operation to malfunction. The simulation of this aspect was carried out using COMSOL Multiphysics, as detailed below. Furthermore, if the quantity of ink dispensed from the nozzle varies, the final printed part may exhibit porosity. To determine whether the pressure exerted by the ink during the initial and final stages of ejection from the nozzle could potentially harm the system, pressure measurements were taken. These measurements were crucial for making decisions regarding the system's integrity.

2. Methods

The device, capable of movement along three axes (X, Y, Z), utilizes ball screws to convert the stepper motor's rotational motion into linear motion. The stepper motor's precise movement accuracy of 1.8 degrees per pulse *allows* for direct coupling with the ball screws, which have a pitch of 5 mm and an external diameter of 16 mm. Each pulse sent to the motor results in a displacement of 0.025 mm along each axis. To maintain linear movement, the device incorporates artificial rails and wagons as linear guides.

Manufactured and assembled with CNC machines and precision instruments, the device features a fixed table where the X, Y, and Z axes are positioned.

Regarding the printing mechanism, the machine's print head is equipped with two nozzles: one for injecting the main material and the other for delivering the support material. With a nozzle diameter of 25 micrometers, the main material consists of quantum dot nanoparticles of copper, carbon, or other substances dispersed in a solution of PVA and ethanol. On the other hand, the support material, PVA (Poly Vinyl Alcohol), dissolves in two solvents: methanol and water.

Beneath the substrate lies a heated bed that allows for the evaporation of methanol in the main material. The heat bed can be heated up to 80 °C. After the coating process, a UV lamp solidifies the quantum dot materials. After printing, the part undergoes a water-washing process to dissolve the support material and PVA within the main component.

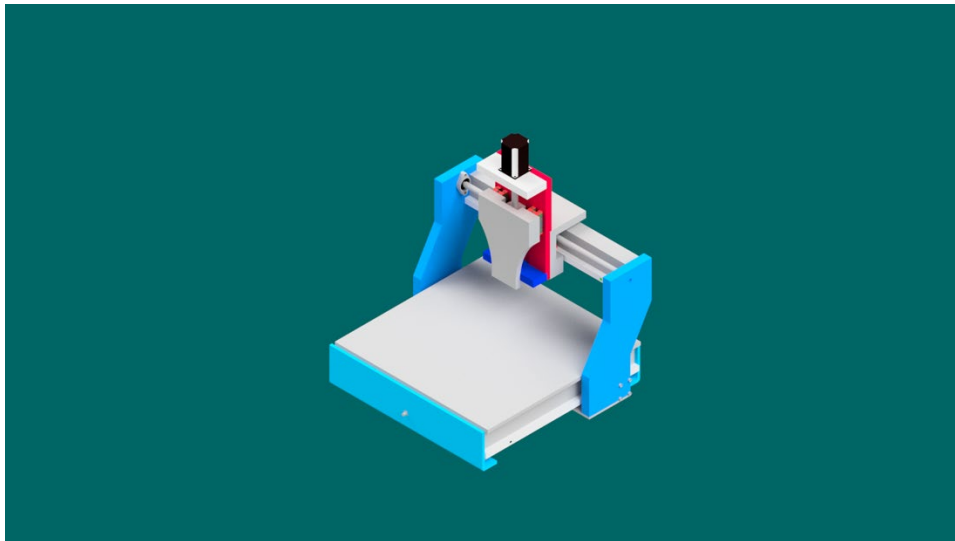


Figure 4: A schematic view of the developed device

3. Discussion

In this study general specifications of the nozzle are as follows:

Considering that the accuracy of the system's movement is 0.25mm, a nozzle has been designed to be compatible with the device's conditions. The nozzle inlet diameter is 5mm and the nozzle outlet diameter is 0.25mm.

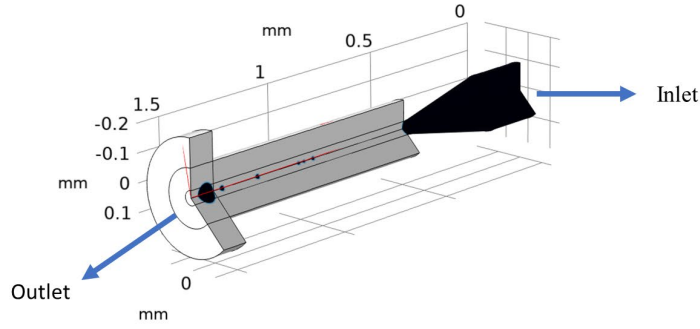


Figure 5: Structure of Nozzle with Outlet and Inlet

It was attempted to simulate the behavior of the ink in the nozzle using the COMSOL Multiphysics software and measured the mass of the output droplet based on the defined values.

It should be noted that the Developed Velocity Profile (Eq.1) was related to the flow velocity variation along a nozzle or pipe. This relationship was derived based on Bernoulli's principle and the law of mass conservation. The Developed Velocity Profile equation as shown in equation 1 was used to calculate the velocity at any point in the nozzle or pipe. The Developed Velocity Profile in this simulation was as follows:

$$\text{Equation 1:} \quad v = 4.5 \left(\frac{r + 5 \text{ mm}}{0.25 \text{ mm}} \right) \left(1 - \frac{r + 5 \text{ mm}}{0.25 \text{ mm}} \right) \text{ m/s}$$

In this analysis, our goal was to reach the maximum output velocity within 2 microseconds, maintain a constant velocity for 10 microseconds, and then reduce the output velocity to zero within 2 microseconds.

In other words, the velocity was increased from zero to 2 microseconds. It was remained constant from 2 to 12 microseconds and then reached zero from 12 to 14 microseconds. Since the fluid exited the nozzle in the form of droplets, a step function was used.

The Smooth Step function as shown in equation 2 is a mathematical function used to transition a value between two specified values. This function creates a smooth and continuous transition from an initial value to a final value through a combination of linear and nonlinear functions. The Smooth Step function was commonly used in computer graphics and simulations. It had two input parameters: an input value (between 0 and 1) and two specified values (usually 0 and 1).

$$\text{Equation 2:} \quad v(r, t) = (\text{step}(t - 1 \cdot 10^{-6}) - \text{step}(t - 13 \cdot 10^{-6})) \cdot v(r)$$

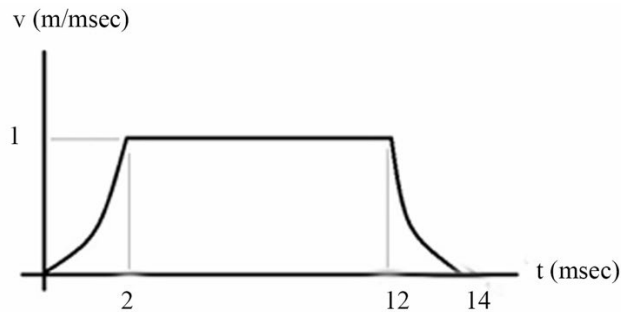


Figure 6: Smooth Step Function Used to Transition a Value Between Two Specified Values.

The goal of this simulation was to get the mass of droplet ink. To perform this simulation, the values of the dynamic velocity and density of the inks were needed and used for printing. These values are specified in the table 1.

Table 1: Density of Inks Over Dynamic Velocity

Matters	Density of Matters
ABS plastic	1.04
Acetone	0.784
Graphite nanoparticles	2.26
Density of ink	0.94

Materials combined in specific percentages as shown in table 2. Since acetone is a solvent for ABS, the dissolution of ABS in acetone resulted in the formation of a suspension consisting of graphite, acetone, and ABS particles. To maintain the dispersion of graphite particles and achieve homogeneous ink, it was necessary to install an ultrasonic shaker in both the ink reservoir and the nozzle outlet.

Finally, the mass of the output droplet was measured by integrating the product of density and droplet volume as shown in Figure 8.

Table 2: Percentage composition of ingredients

Matters	Percentage of Matters
ABS plastic	11.86 %
Acetone	79.37 %
Graphite Powder	8.77 %

The objective of this experiment is to develop a conductive ink suitable for use in a 3D printing device, requiring printability and compatibility with a nozzle. In this investigation, ABS serves as a binder for graphite particles, forming a liquid polymer glue when dissolved in a solvent like acetone. However, the initial ABS-acetone solution lacks conductivity. Table 2 demonstrates that by incorporating 8.77% graphite, a conductive solution with a resistance of 108 ohms can be achieved. The subsequent focus is on evaluating the printability of the ink. Using COMSOL Multiphysics, various parameters are assessed to ensure the ink is nozzle-friendly and suitable for printing.

To emulate real conditions accurately, an ultrasonic shaker is employed, counteracting the assumption of homogeneity in COMSOL Multiphysics. Without the use of the ultrasonic shaker, graphite particles tend to settle over time, creating a disparity between simulated and actual ink conditions. Acetone, employed solely for suspension purposes, necessitates removal after lithography on the substrate. To address this, a heater beneath the substrate, capable of reaching 80 °C, ensures the evaporation of acetone. Since the liquefaction temperature of ABS is 240 °C, this heat doesn't compromise the substrate layer, facilitating the swift removal of acetone from the materials.

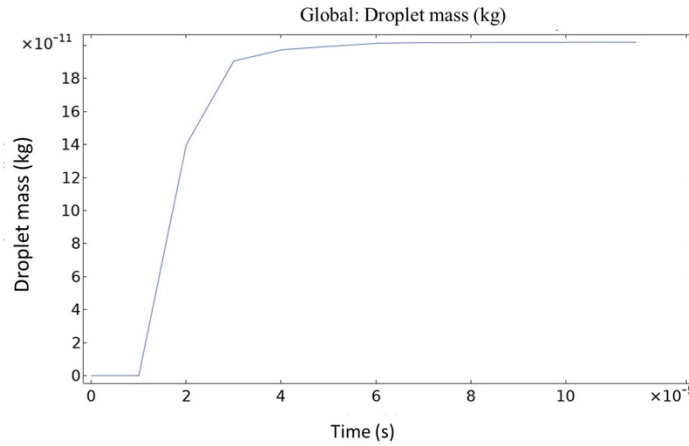


Figure 7: The mass of the droplet ejected from the nozzle as a function of time

In Figure 7, the weight of the output droplet is specified. The vertical axis represents the weight of the droplet in Kg E-11, and the horizontal axis represents the elapsed time. Based on the obtained results, it can be concluded that the weight of the output droplet becomes constant after 50 E-6 seconds. The weight of the output droplet was calculated using the definition of material density used in the COMSOL Multiphysics software. The materials used and their densities can be seen in Table 1. From the information in Figure 7, it was inferred that during the printing process, it was uniform spraying, and expected a uniform printed product as well.

Due to acetone being a solvent for ABS, ABS is dissolved in acetone, resulting in a suspension of graphite particles, acetone, and ABS at the end. To ensure that graphite particles remain dispersed and a homogeneous ink exists, an ultrasonic shaker is needed to install in the ink reservoir and at the nozzle outlet.

In Figure 8, It can be observed the ink pressure profiles, with the horizontal and vertical axes representing the cross-sectional surface in millimeters. In Figure 8a, the ink pressure at time 2E-4 is visible, which corresponds to the moment the ink exits the nozzle. The pressure values in pascals (Pa) are displayed in the color-coded column next to the graph. In Figure 8b, the pressure value at T=0 is shown, which is also 0. Based on the obtained results, the maximum pressure that the nozzle can withstand is 2.91E-4 Pa.

In Figure 8, the size of the droplet velocity is visible. The vertical and horizontal axes of the graph represent the cross-sectional surface of the nozzle in millimeters. By referring to the legend of the graph, located on the right side of each figure, you can observe the magnitude of the velocity. In Figure 8c, the magnitude of the droplet velocity at the moment of exiting the nozzle is displayed, with a maximum size of 6E-3 m/s. In Figure 8d, the magnitude of the velocity at the starting time T=0 is visible, and according to the graph, its value is 0.

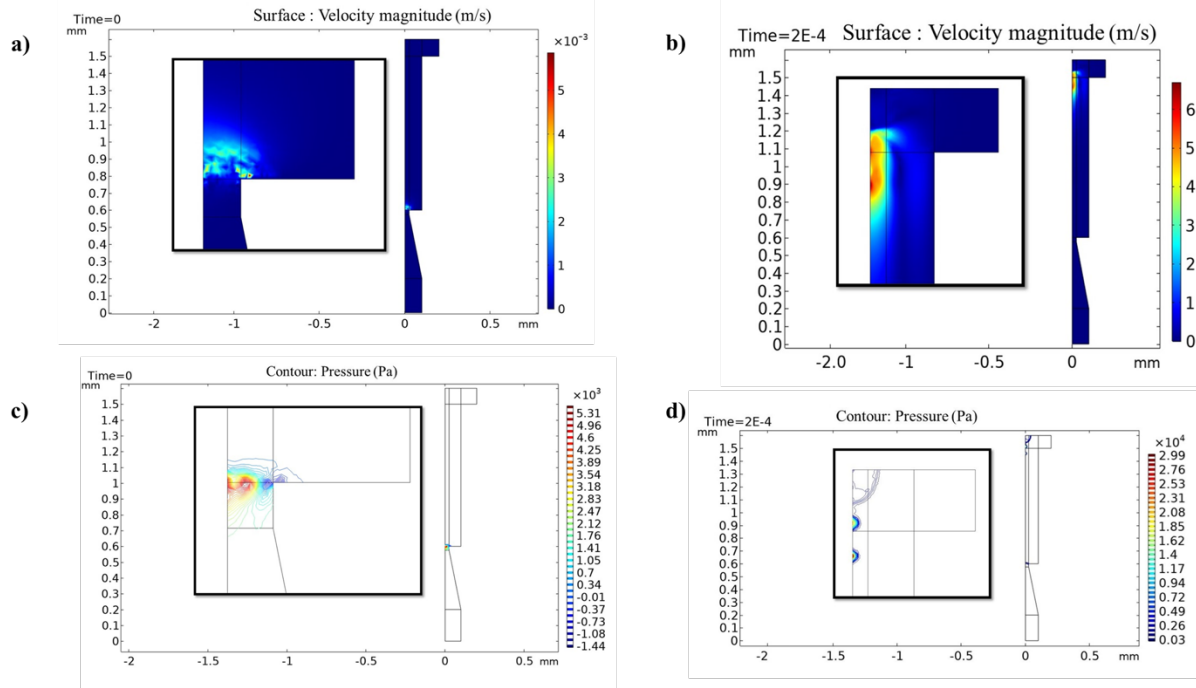


Figure 8: Ink Pressure Profile, (a) the moment ink exits the nozzle at $2E-4$ is visible, and (b) the maximum pressure nozzle can withstand is $2.91E-3$ Velocity Graph- (c)- the magnitude of the droplet velocity at the moment of exiting the nozzle is $6E-3$ m/s and (d) the magnitude of the velocity at $T=0$ is visible, its value is 0.

4. Conclusion

In conclusion, our study demonstrates inkjet printing technology's newfound potential in versatile applications spanning from material engineering to medical fields. While tackling challenges related to 3D geometries and material properties, we have examined in depth the significant role of support structures, ink viscosity, and advanced technologies such as heaters and ultrasonic systems.

Our research focused on optimizing the structural complexity through a specifically designed nozzle adapted to our system's movement accuracy of 0.25mm. The simulation of the ink behavior inside this nozzle, performed with the COMSOL Multiphysics software, sheds light on the inherent intricacies of the ink's density, dynamic velocity, and droplet formation.

In particular, we discussed the application of the Developed Velocity Profile equation and the Smooth Step function to attempt to control the ink flow rate to achieve our targeted timing parameters. The research further compounds the role of specific material properties like the density and dynamic velocity of ABS plastic, acetone, and graphite nanoparticles in ensuring the best output from our designed system.

Our innovative approach introduces a mixture of ABS plastic, acetone, and graphite nanoparticles, combining them under carefully proportioned quantities to ensure a homogeneous ink. The study emphasizes the introduction of an ultrasonic within the ink reservoir and at the nozzle outlet, a step pivotal to maintaining a steady dispersion of graphite particles.

We illustrate the conductivity of ABS polymer in three stages, followed by an examination of ink printability. Finally, we simulate the deposited layer to determine its conductivity. Our findings reveal that ABS exhibits conductivity, our ink is successfully printable, and the deposited layer also demonstrates conductivity.

The pioneering methodology highlighted in this study could provide an impetus for multitudes of applications: additive manufacturing processes, and a more comprehensive range of printable materials, to name a few future directions. The effort to replace conventional coating methodologies with superior printing techniques revolutionizes many sectors and sets a new benchmark for printing technology.

5. References

- [1] I. Gibson, D. Rosen, and B. Stucker, *Additive Manufacturing Technologies*. New York, NY: Springer New York, 2015. doi: <https://doi.org/10.1007/978-1-4939-2113-3>.
- [2] E. A. Clark *et al.*, “3D printing of tablets using inkjet with UV photoinitiation,” *International Journal of Pharmaceutics*, vol. 529, no. 1–2, pp. 523–530, Aug. 2017, doi: 10.1016/j.ijpharm.2017.06.085.
- [3] T. Ngo, A. Kashani, G. Imbalzano, Q. T. Nguyen, and D. Hui, “Additive manufacturing (3D printing): A review of materials, methods, applications and challenges,” *Composites Part B: Engineering*, vol. 143, pp. 172–196, Jun. 2018, doi: 10.1016/j.compositesb.2018.02.012.
- [4] G. Baldini, A. Albini, P. Maiolino, and G. Cannata, “An atlas for the inkjet printing of Large-Area tactile sensors,” *Sensors*, vol. 22, no. 6, p. 2332, Mar. 2022, doi: 10.3390/s22062332.
- [5] M. Yousefizad, M. M. Ghezelayagh, S. Hooshmand, and F. Raissi, “Fabrication and characteristics of double heterojunction bipolar transistor based on p-CuO/n-Si heterojunction,” *Applied Nanoscience*, vol. 12, no. 11, pp. 3637–3645, Jul. 2022, doi: 10.1007/s13204-022-02545-z.
- [6] M. Yousefizad *et al.*, “Performance investigation of low-power flexible n-ZnO/p-CuO/n-ZnO heterojunction bipolar transistor: Simulation study,” *Micro and Nanostructures*, vol. 180, p. 207594, Aug. 2023, doi: 10.1016/j.micrna.2023.207594.
- [7] P. Ghamari, F. Raissi, and N. Manavizadeh, “low cost schottky barrier solar cells based on cuo fabricated by sputtering method,” in *2nd International Conference and eExhibition on Solar Energy (ICESE)*, Tehran, Iran, 2015.
- [8] N. H. Raad, E. Karimmirza, M. Yousefizad *et al.*, “Improving the electronic and optical properties of chalcogenide Cu₂ZnSnS₄ compound with transition metal dopants: A first-principles investigation,” *Thin Solid Films*, vol. 766, p. 139653, 2023.
- [9] N. Nouri, T. Ghafouri, Z. G. Bafghi, N. Manavizadeh, and M. A. Zeidabadi, “A First-Principles study on the electronic and optical properties of ZnO nanowires toward detection of α -Amino acids,” *Journal of Photochemistry and Photobiology A: Chemistry*, 2023, Art. no. 115237.
- [10] T. Ghafouri and N. Manavizadeh, “A 3D-printed millifluidic device for triboelectricity-driven pH sensing based on ZnO nanosheets with super-Nernstian response,” *Analytica Chimica Acta*, vol. 1267, pp. 341342, 2023.
- [11] S. S. Golpaygani *et al.*, “Modification of Dye-Sensitized Solar Cells by SWCNT Composition as the Active Layer and Introducing TiO₂@ SiO₂ Core–Shell Nanostructure for Light Scattering Layer: Toward Efficiency Enhancement,” *IEEE Transactions on Electron Devices*, vol. 70, no. 5, pp. 2437–2444, 2023.
- [12] Z. G. Bafghi and N. Manavizadeh, “Low power ZnO nanorod-based ultraviolet photodetector: effect of alcoholic growth precursor,” *Optics & Laser Technology*, vol. 129, p. 106310, 2020.
- [13] M. Nourafkan and N. Manavizadeh, “The Effect of Nanowire Dimensions on Resonance Frequency of ZnO-Based Nanogenerator,” in *2019 27th Iranian Conference on Electrical Engineering (ICEE)*, pp. 190–194, IEEE, 2019.
- [14] N. Manavizadeh *et al.*, “Performance assessment of nanoscale field-effect diodes,” *IEEE Trans. Electron Devices*, vol. 58, no. 8, pp. 2378–2384, 2011.
- [15] M. Yousefizad, S. Hooshmand, M. M. Ghezel-Ayagh, and F. Raissi, “Two-dimensional physical and numerical modeling of copper (II)-oxide/silicon hetero junction bipolar transistor,” *Advanced Ceramics Progress*, vol. 7, no. 2, pp. 28–33, 2021.
- [16] M. Yousefizad, S. Rezaei, A. M. Shahriyari, M. M. Ghezel-Ayagh, S. Hooshmand, N. Manavizadeh, “High-performance copper oxide-based heterojunction bipolar transistor: design, modeling, and performance analysis,” *Journal of Characterization*, vol. 3, no. 3, Dec 2023, doi: 10.29228/JCHAR.73922

- [17] M. A. Shah, D.-G. Lee, B. Lee, and S. Hur, "Classifications and Applications of Inkjet Printing Technology: a review," *IEEE Access*, vol. 9, pp. 140079–140102, Jan. 2021, doi: 10.1109/access.2021.3119219.
- [18] K. Zub, S. Hoepfner, and U. S. Schubert, "Inkjet printing and 3D printing strategies for biosensing, analytical, and diagnostic applications," *Advanced Materials*, vol. 34, no. 31, Jun. 2022, doi: 10.1002/adma.202105015.
- [19] P. Delrot, M. A. Modestino, F. Gallaire, D. Psaltis, and C. Moser, "Inkjet printing of viscous monodisperse microdroplets by Laser-Induced flow focusing," *Physical Review Applied*, vol. 6, no. 2, Aug. 2016, doi: 10.1103/physrevapplied.6.024003.
- [20] L. D. Garma, L. M. Ferrari, P. Scognamiglio, F. Greco, and F. Santoro, "Inkjet-printed PEDOT:PSS multi-electrode arrays for low-cost *in vitro* electrophysiology," *Lab on a Chip*, vol. 19, no. 22, pp. 3776–3786, Jan. 2019, doi: 10.1039/c9lc00636b.
- [21] H. Wijshoff, "The dynamics of the piezo inkjet printhead operation," *Phys. Rep.*, vol. 491, nos. 4–5, pp. 77–177, Jun. 2010.
- [22] S. Guddati, A. S. K. Kiran, M. Leavy, and S. Ramakrishna, "Recent advancements in additive manufacturing technologies for porous material applications," *The International Journal of Advanced Manufacturing Technology*, Aug. 2019, doi: <https://doi.org/10.1007/s00170-019-04116-z>.